Neural Computing and Applications (2020) 32:6343–6351
https://doi.org/10.1007/s00521-019-04142-8

ORIGINAL ARTICLE

Surface EMG hand gesture recognition system based on PCA and GRNN

Jinxian Qi[1] · Guozhang Jiang[2,4] · Gongfa Li[3,4] · Ying Sun[1,2] · Bo Tao[1,3]

Received: 29 August 2018 / Accepted: 9 March 2019 / Published online: 15 March 2019

Abstract
The principal component analysis method and GRNN neural network are used to construct the gesture recognition system, so as to reduce the redundant information of EMG signals, reduce the signal dimension, improve the recognition efficiency and accuracy, and enhance the feasibility of real-time recognition. Using the means of extracting key information of human motion, the specific action mode is identified. In this paper, nine static gestures are taken as samples, and the surface EMG signal of the arm is collected by the electromyography instrument to extract four kinds of characteristics of the signal. After dimension reduction and neural network learning, the overall recognition rate of the system reached 95.1%, and the average recognition time was 0.19 s.

Keywords sEMG · Gesture recognition · Feature reduction · PCA · GRNN · Machine learning

1 Introduction

Surface EMG reflects the activity state of the nerve, it can be analyzed to push back the neural information, and the surface EMG signal has the advantages of noninvasive acquisition, bionics, etc., so it is well in the fields of prosthetic control, clinical diagnosis, motion detection, and neurological rehabilitation [1, 2]. Gesture recognition based on surface EMG signals is an important research topic in the practical application of surface EMG, and reliable and effective gesture recognition can help develop a good human–machine interface.

✉ Gongfa Li
ligongfa@wust.edu.cn

1 Key Laboratory of Metallurgical Equipment and Control Technology of Ministry of Education, Wuhan University of Science and Technology, Wuhan 430081, China

2 Hubei Key Laboratory of Mechanical Transmission and Manufacturing Engineering, Wuhan University of Science and Technology, Wuhan 430081, China

3 Research Center of Biologic Manipulator and Intelligent Measurement and Control, Wuhan University of Science and Technology, Wuhan 430081, China

4 Institute of Precision Manufacturing, Wuhan University of Science and Technology, Wuhan 430081, China

There is a relationship between the sEMG signal and the limb movement. Muscle contraction or relaxation causes different limb movements, and a large difference in bioelectrical signals is released [3, 4]. Feature extraction by sEMG signal and then analysis of features can be pushed to the active state of the muscle, thereby identifying the action pattern resulting from muscle contraction [5–8].

An auxiliary device for controlling neurological rehabilitation (for example, an active prosthesis) is realized through a human–machine interface. When detecting neuromuscular system information, interfaces can be connected to the brain, peripheral nerves, and muscle regions [9–13], among these potential options, muscle interface is currently the only viable method for controlling external devices in commercial and clinical systems [14, 15, 16]. Due to its noninvasive, relatively simple application, and rich neural information, surface EMG signals can be widely used in human–machine interfaces which can control prostheses in clinical and commercial fields [17, 18].

Studies have shown that human limb movement is a joint movement of muscles and bones controlled by the nervous system, so different peoples have different habitual exercise patterns [19, 20], even the same person has different modes of motions under different external conditions and different physical and psychological conditions. This

puts high demands on EMG signal processing and feature extraction.

In addition, because the EMG signal is more complex, the performance requirements of the system are higher, and the response time of the pattern recognition system is slower, which has adverse effects on real-time prosthetic control or other applications [21–23].

In view of the above problems, based on the previous research, this paper uses the means of extracting the key information of human body motion to identify the specific action mode and takes the specific gesture as a sample to extract the feature of the acquired surface EMG. Use PCA to reduce feature dimensions and eliminate redundant information and construct the GRNN neural network classifier to achieve the purpose of accurate pattern recognition, which is of great significance for the development of prosthetic control, clinical medicine, brain health, human–computer interaction, and other fields.

2 Feature extraction

After the EMG signal is segmented through the window, feature extraction can be performed on the intercepted signal in a single window. The properties of the extracted features affect the performance of the gesture recognition system, for example, the number and type of features affect the real-time accuracy of the system. In the field of signal analysis, the types of features are mainly time-domain features, frequency-domain features, time–frequency features, and nonlinear methods. According to the research results of the reference, only two time domain features, root mean square (RMS) and wavelength (WL), can obtain good classification results [24–26]. In addition, the median amplitude spectrum (MAS) and sample entropy (SampEn) are introduced [27–31]. Therefore, this study uses these four parameters as extracted features.

2.1 Acquisition of signal sets

This paper uses the electromyograph which has advanced surface EMG signal amplification technology and 16-channel high space-time resolution sampling technology. As shown in Fig. 1, the electrode sleeve can be used to quickly and easily collect the arm muscle signal. Among them, 18 dry electrode sheets are placed, among which the electrodes 1–16 are sampling electrodes, 17 is the reference electrode, and 18 is the bias electrode.

As shown in Fig. 2, according to the research results of Xiong Caihua [26], Fang Yinfeng [32], and other people [33–36], 9 hand movements were planned for sEMG data collection. The 9 gestures involve the whole hand exercise, including palm closure (SH) and palm open (SK), wrist movement including wrist flexion (NQ) and external flexion (WQ), finger movement including thumb force on index finger (MS), middle finger (MZ), ring finger (MW), and the little finger (MX) and in addition to this test gesture action also include a rest action (RE). In each experiment, 10 trials were repeated for each action. The repeated method is to rest for 5 s, keep the action for 5 s, repeat 10 times, and collect for 3 consecutive days, using the same collection method every day. This method can be used to obtain temporal and spatial differences in myoelectric signals of the same individual.

Fig. 1 Electrode sleeve

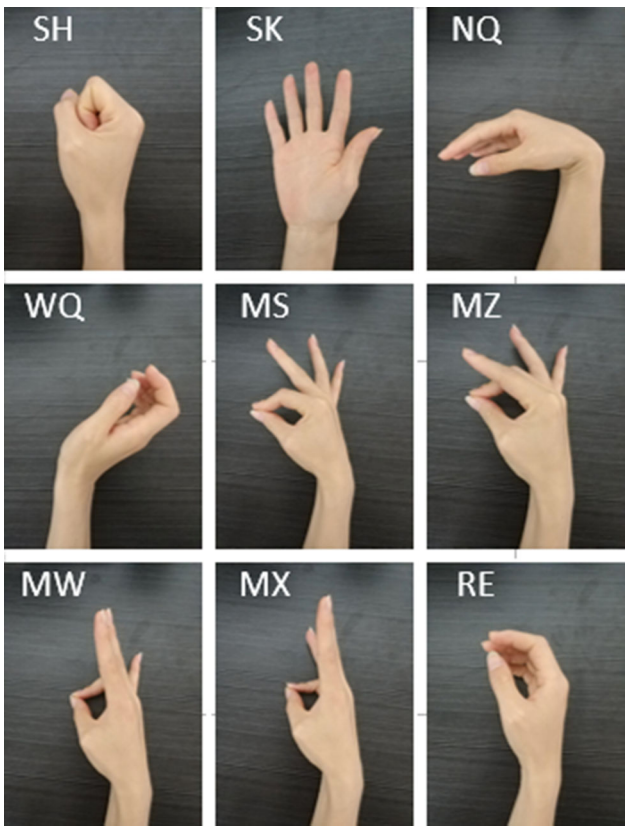

Fig. 2 Static gesture

2.2 Time-domain characteristics

1. Root mean square (RMS) is the measure of the amplitude of the EMG signal, which can be expressed as:

$$\mathrm{RMS} = \sqrt{\frac{1}{N}\sum_{i=1}^{N} x_i^2} \tag{1}$$

where N is the length of the window and is the i th sample point. Similar to RMS, the absolute value of the integral and the mean absolute value (MAV) have been proven to have the same performance in manual identification. Therefore, this paper chooses RMS as the representative.

2. Waveform length (WL) refers to the cumulative length of the EMG waveform. Its principle is:

$$\mathrm{WL} = \sum_{i=1}^{N-1} |x_{i+1} - x_i| \tag{2}$$

where N is the length of the window and i is the ith sample point.

2.3 Frequency-domain characteristics

The median amplitude spectrum (MAS) reflects the relationship between the amplitude and frequency of a wave or wave train. The MAS feature can ignore the extreme value, so it reflects the average characteristics of the signal in the frequency domain. The principle of the median amplitude spectrum is as follows:

$$\mathrm{MAS} = \frac{1}{2} \times \sum_{i=1}^{N} \left| \frac{\mathrm{FFT}(S)}{L} \right| \tag{3}$$

where S is a segment of the original signal, N is the length of the window, L is the length of the signal, and FFT is the fast Fourier transform.

2.4 Sample entropy

SampEn (sample entropy) is a method of measuring the complexity of time series. Its sample entropy can be expressed as SampEn(m, r, N), where N is the length of time and r is similar tolerance; dimensions are defined as m and $m + 1$. The sample entropy is used to reduce the error of the approximate entropy and is closer to the existing random part [4, 37, 38].

When N is finite, the equation is expressed as:

$$\mathrm{SampEn}\ (m, r, N) = -\ln \frac{B^{m+1}(r)}{B^m(r)} \tag{4}$$

Among them, $B^m(r) = L/(N - m - 1)$

$$d_{x(i)x(j)} = \max_k \left(\left| x_{(i+k)} - x_{(j+k)} \right| \right) \quad k = 0, \ldots, m-1$$

For a given threshold r, for each i, the number of occasions whenever $d_{x(i)x(j)}$ is less than r is specified as the number of template matches represented by L, and the ratio of the number to the total number of distance $d_{x(i)x(j)}$ is expressed as $B_i^m(r)$.

3 Feature dimensionality reduction based on PCA

The training of the pattern classifier for EMG signals depends on the large training database, but these multifarious data reduce the training speed of the model, so the highly efficient features or channel data will be selected from it, but it has great uncertainty for different gestures or collection methods. There are different combinations of requirements, and if a large portion of the information is lost in the sample arrangement, the coupling situation will occur, which leads to a large reduction in the classification ability of the classifier [39, 40]. Therefore, it is necessary to improve the efficiency of data utilization by means of dimensionality reduction, and avoid overloading of the classifier [41, 42]. In addition, dimensionality reduction can eliminate redundant information and prevent non-essential information from interfering with the correct judgment of the classifier. Therefore, when we do a lot of pattern recognition, we need to introduce the method of feature dimensionality reduction [43, 44].

For the problem of reducing the dimension of high-dimensional signals, the strategy is to assume that the data are linearly separable in low-dimensional space, and the main representative algorithm is the principal component analysis (PCA) [45]. The algorithm has developed a complete theoretical system, and has shown good performance in practical applications.

3.1 PCA principle

In the basic idea of principle component analysis (PCA), a small number of new variables (linear combinations of the original variables) are used instead of the original variables [46–49]. The new variable should reflect the signal information of the original variables to the maximum extent, and at the same time, the new variables are orthogonal to each other and can be used to eliminate the overlapping information in the original variables.

The standardized input variable matrix of the sample is as follows:

$$X = \begin{bmatrix} x_{11} & x_{12} & \cdots & x_{1k} \\ x_{21} & x_{22} & \cdots & x_{2k} \\ & & \cdots & \\ x_{n1} & x_{n2} & \cdots & x_{nk} \end{bmatrix} \tag{5}$$

It is required to construct a variable P_1 to meet the following conditions:

$$P_1 = Xt_1,\ \|t_1\| = 1 \tag{6}$$

On the other hand, the variables are enabled to carry information that normalizes the input variable matrix $X_{n\times k}$.

From the viewpoint of probability and statistics, the greater the variance of a variable, the more information it carries. Therefore, the above problems can be transformed into the maximum variance of the required variables. P_1 variance is

$$\mathrm{Var}(P_1) = \frac{1}{n}\|P_1\|^2 = \frac{1}{n}t_1' X' X t_1 = t_1' \quad Vt_1 V = \frac{1}{n}X'X \tag{7}$$

Constructing a Lagrangian function

$$L = t_1' V t_1 - \lambda(t_1' t_1 - 1) \tag{8}$$

Among them, λ_1 is the Lagrangian coefficient. To calculate the partial derivatives of L to λ_1 and t_1 separately and make them zero, there are the following rules:

$$\begin{cases} \dfrac{\partial L}{\partial t_1} = 2Vt_1 - 2\lambda_1 t_1 = 0 \\ \dfrac{\partial L}{\partial \lambda_1} = -(t_1' t_1 - 1) = 0 \end{cases} \quad Vt_1 = \lambda_1 t_1 \tag{9}$$

It can be seen that t_1 is a normalized feature vector of V, and λ_1 is its corresponding feature value

$$\mathrm{Var}(P_1) = t_1' V t_1 = t_1' \lambda_1 t_1 = t_1' t_1 \lambda_1 = \lambda_1 \tag{10}$$

The required t_1 is the normalized feature vector corresponding to the maximum eigenvalue λ_1 of the matrix V. The corresponding structural variable $P_1 = Xt_1$ at this time is called the first principal component.

By analogy, the m th principal component of V can be found as $P_m = Xt_m$.

The sum of the information carried by the former m principal components is:

$$\sum_{i=1}^{m} \mathrm{Var}(P_i) = \sum_{i=1}^{m} \lambda_i \tag{11}$$

The data dimension obtained by transforming in the new coordinate space is the same as the data dimension of the original space. It is worth noting that the variance of the data in the new coordinates mainly exists in previous several dimensions, so we can achieve the purpose of dimensionality reduction by retaining only the principal components of the first few dimensions.

3.2 Pretreatment

The feature data need to be preprocessed before dimension reduction, in order to unify the order of magnitude of each feature parameter. Because the magnitude of each feature parameter is different, even a big difference. As shown in Fig. 3, it can be seen that the WL features are of the largest order from Fig. 3a, and other features are covered when gesture recognition is performed. The classifier is sensitive to large values of data, ignoring other features, so the features need to be normalized.

The feature values are mapped into the (0, 1) space by min–max normalization shown in part b of Fig. 3. So the features are in the same order of magnitude, and the features can be merged without overlapping each other, while simplifying the calculation.

3.3 Way of dimensionality reduction

This paper uses four features to be integrated into one feature set. The feature set includes root mean square (RMS), wavelength (WL), sample entropy (SampEn), and median amplitude spectrum (MAS) for a total of 64 dimensions (16 channels × 4 features).

In the experiment, after the 64 feature set is analyzed by the principal component analysis, a new 64-dimensional feature set which is arranged according to the variance of the components is formed. Then, the first n dimensions of the new feature set are taken as the reduced dimension feature set. The value of the dimensional k after the optimal dimensionality reduction is determined by the calculated principal component ratio which should be above 95%.

As shown in Fig. 4, the contribution rate of the first three principal components is accounted for, and the first three accumulative accounts are 98.3%. Therefore, k value of this experiment is 3, and the first three principal components are taken as the new dimensionality reduction eigenvectors.

Before the classification, the training components and the first two components of the test set are compared, as shown in Fig. 5.

It can be found that the first and second principal components of the test set and the training set are substantially coincident, and the classification effect is best when the main component of the training set is included in the test set.

As shown in Fig. 6, these two images show the feature separation before and after PCA processing, and according to the value of k, the first three features are also taken before dimension reduction. As shown in Fig. 6a,

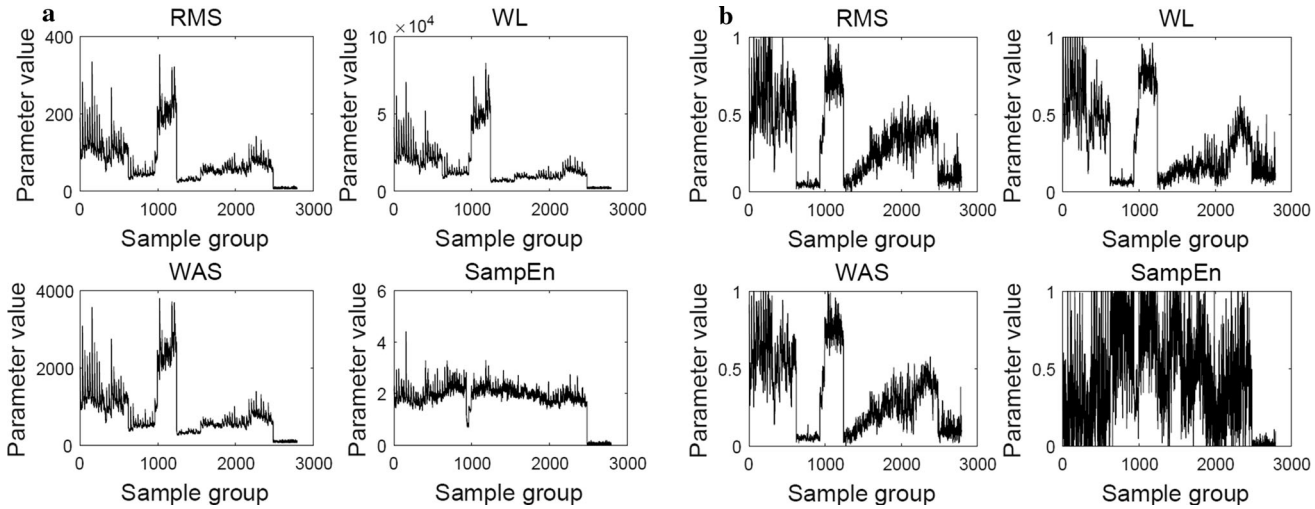

Fig. 3 Comparison of single channel eigenvalues before and after normalization

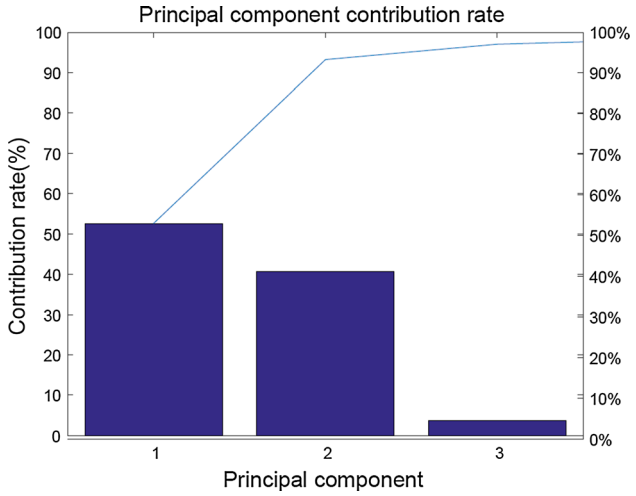

Fig. 4 Principal component contribution rate

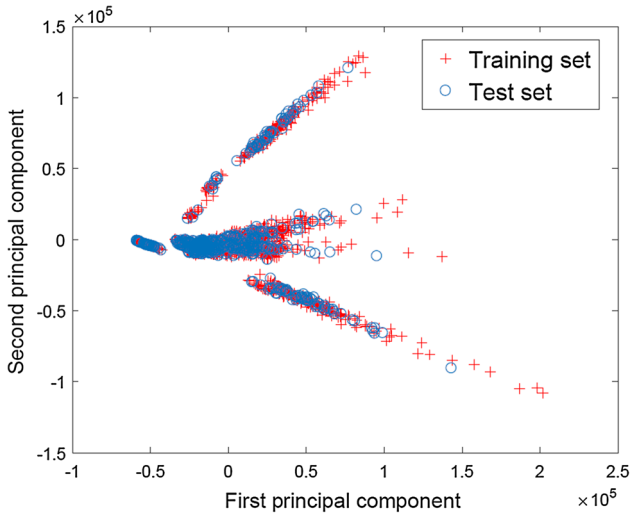

Fig. 5 Principal component analysis of training set and test set

obviously, each gesture cannot be distinguished well. As shown in Fig. 6b, the first three features which have the principal component are used to test feature separation. The divergence of the scatter plot for each gesture is very high, and it is clear that they can be effectively distinguished.

4 GRNN neural network classifier

4.1 GRNN network principle

The GRNN network proposed by Specht [50] is a variant of a radial basis neural network and is commonly used for approximation functions. As a generalization of radial basis function (RBF) and probabilistic neural network (PNN) networks, GRNN networks do not require an iterative process for training and high degree of parallelism are presented in their structure. This network can be used for predictive modeling, mapping, and interpolation or as a controller [51–54].

The architecture of the GRNN network is shown in Fig. 7. The input layer receives a vector X containing the M input variables of the network. The number of neurons constituting the layer corresponds to the number of training patterns stored in the weight matrix w_1.

When a new vector is input to the network, the distance between the input vector and the vector stored weight is typically calculated in Dist block using the Euclidean distance. The output of block Dist is multiplied by the polarization factor b point by point. The result of this multiplication is applied to the radial basis function provided as output a_1.

The second layer performs the sum of the outputs a_1 according to the number of outputs required. The weight

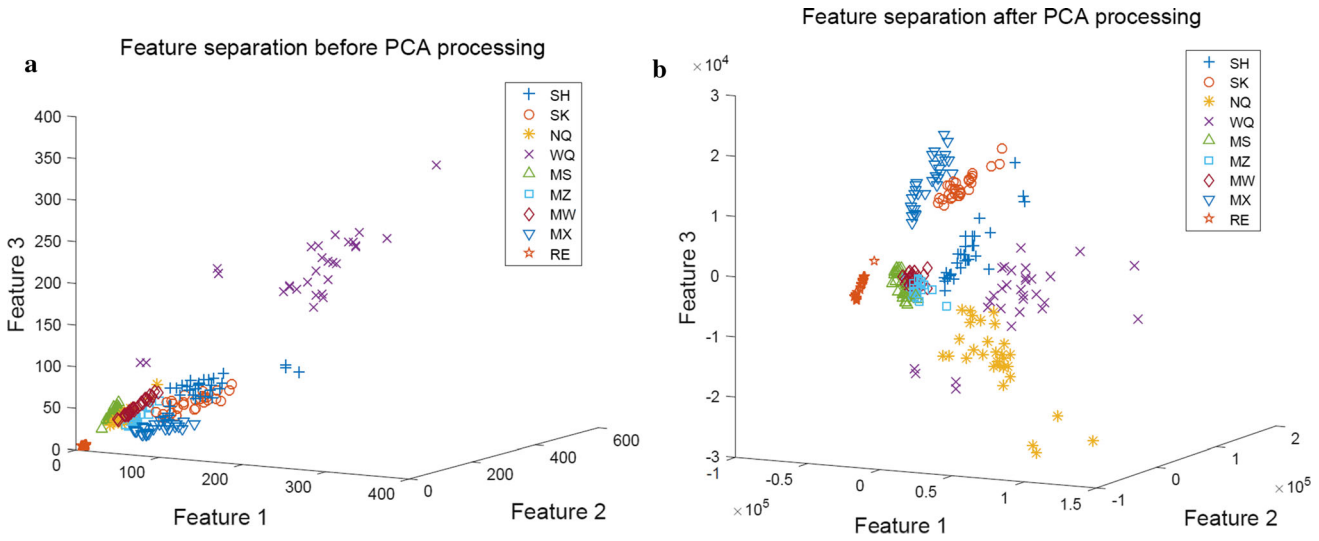

Fig. 6 Comparison of feature separation before and after PCA dimension reduction

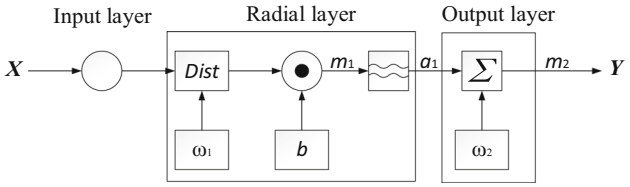

Fig. 7 Schematic diagram of the GRNN network

matrix ω_1 of this layer already stores the target vector containing the desired output. The output vector m_2 is obtained by adding the product of each element of a_1 to the elements of each vector stored in ω_1, normalized by the sum of the elements of a_1. Then, when an input vector X is stored in the network beside the training vector x_i in the first layer, the vector X produces an output a_{1i} close to 1 in the first layer. This results in the output of the second layer being the vector m_{2i} next to it, one of which is stored in the second layer.

The GRNN network has the advantages of simple structure, fast training, and few adjustment parameters. In addition, compared with the feedforward network, the calculation results of the GRNN network have global convergence. So in this paper, GRNN is used as a classifier for supervised gesture recognition.

4.2 Gesture recognition experiment results and analysis

The data are divided into a test set and a training set; the training set is used to train the classifier parameters, and the test set is used to test the classifier training.

1. Identification results before dimensionality reduction

The feature values of each gesture are randomly divided into two groups: one is a training set and one is a test set. The training set contains 250 sets of data for each gesture, and each test set contains 60 sets of data.

The sleeves are collected in a total of 16 channels which are not used as input for pattern recognition at the same time. Instead, 16 channels are arranged in a gradient to construct multiple different combinations of classifiers. According to the arrangement and combination, 136 classifiers are obtained. They are arranged as shown in Fig. 8.

As shown in Fig. 9, the correct rate comparison chart of the 136 classifiers corresponding for the four features. The abscissa of the graph represents the label of 136 models, and the ordinate represents the correct rate of the model.

The correct rate distribution of the four graphs in Fig. 9 can be analyzed, the more the input channels of the classifier, the better the effect of pattern recognition, the less the input channel, the worse the effect of pattern recognition. However, in some cases, the data of each channel affect each other, and too many channels will cause the pattern recognition success rate to decrease.

The accuracy and calculation time of the classifier are evaluated separately. The classification results of the four characteristics are shown in Table 1. The accuracy of the

1～1，1～2，1～3 …… 1～16；
2～2，2～3，2～4 …… 2～16；
……
15～15，15～16；
16～16

Fig. 8 Input channel arrangement

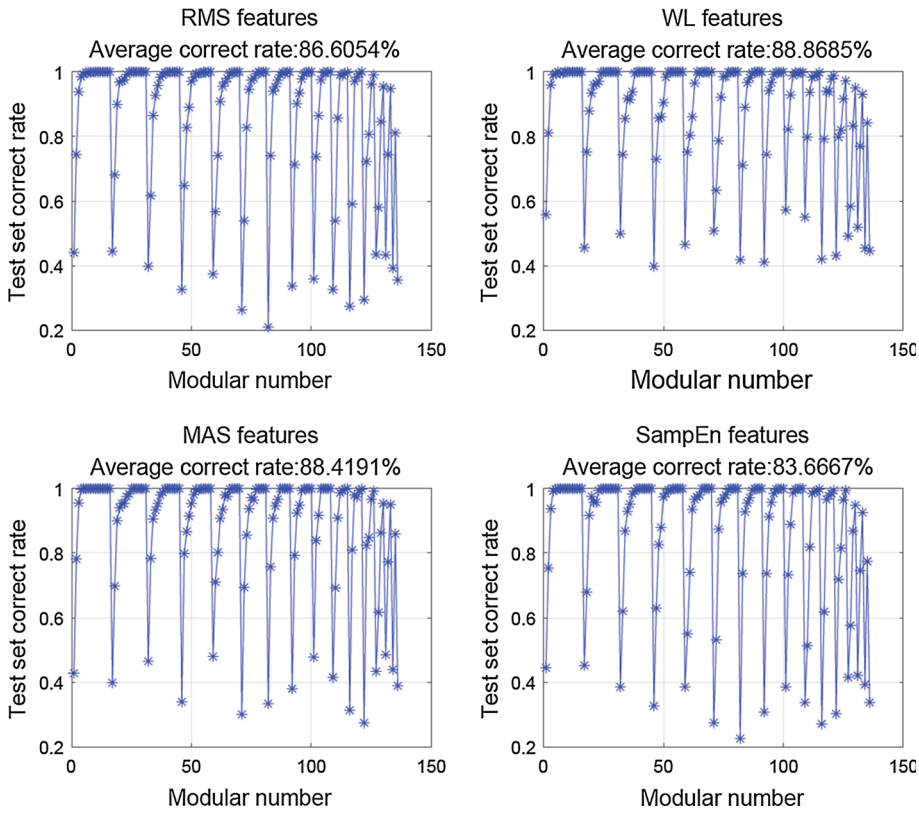

Fig. 9 Accuracy of recognition results for four features

Table 1 Comparison table of feature classification results

Item	RMS	WL	MAS	SampEn
Average accuracy (%)	86.6054	88.8685	88.4191	83.6667
Average running time (s)	0.2553	0.18991	0.22403	0.17762

identification of the four features and the average time of operation are recorded in Table

2. Experimental results after dimensionality reduction

After dimension reduction, the first three principal component features are used for pattern recognition in the GRNN classifier; the correct rate is 95.1%, and the average operation time is 0.19 s, as shown in Figs. 10 and 11. The accuracy of gesture recognition is higher than the average of the success rate of previous individual features.

Principal component analysis is a simple and efficient unsupervised feature dimension reduction method. After the dimensionality reduction process, the feature size can be reduced, the redundant information can be reduced, the accuracy of the pattern recognition can be improved, and the stability of the classifier can be improved. At the same time, the dimensionality reduction method can be used to reduce the structure of the simplified classifier and enhance the real-time performance of the classifier. Compared with other recognition systems, such as BP neural network [2, 22] and D–S evidential theory [3], the method of this paper has greatly improved the recognition efficiency and accuracy.

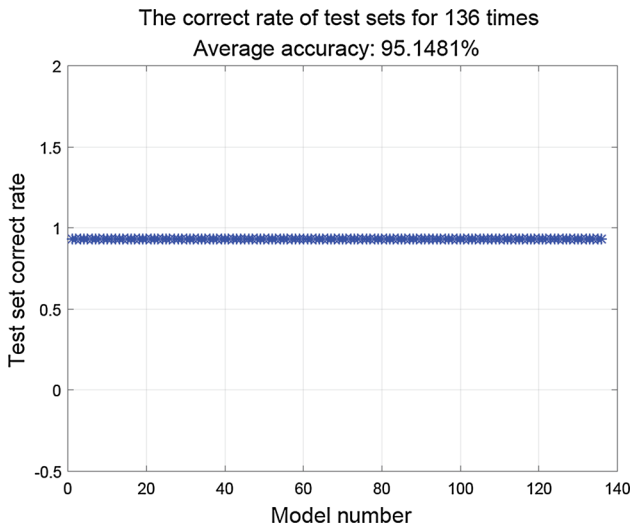

Fig. 10 Identification results after dimensionality reduction

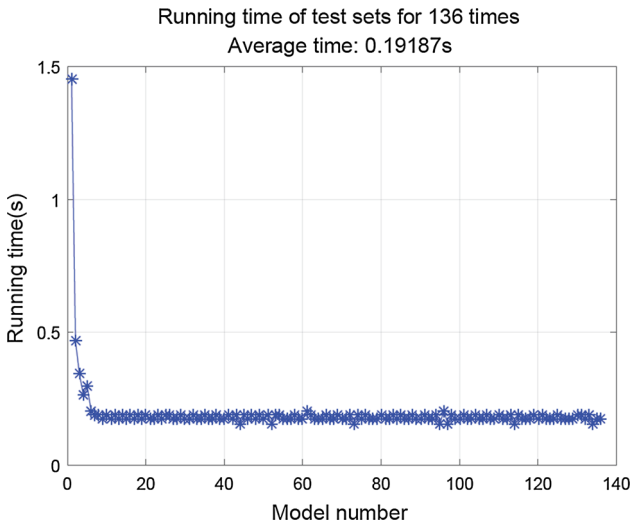

Fig. 11 Average operation time after dimensionality reduction

5 Conclusion

This paper studies the recognition of static gestures based on EMG signals. The main characteristics of surface EMG signals, non-stationary, nonlinear, non-deterministic, etc., make effective feature extraction and pattern recognition difficult. In addition, choosing a fast, simple, and effective pattern classification scheme has become a difficult problem that must be faced before pattern recognition. Based on the extraction of RMS, WL, MAS, and SampEn, this paper reduces the feature dimension and eliminates redundant information by the PCA algorithm. At the same time, the classifier of GRNN generalized regression neural network is constructed to achieve highly efficient and highly accurate static gesture recognition target. The accuracy of the resulting gesture recognition was significantly improved to 95.1%, and the calculation time was only about 0.19 s, which made it possible for real-time processing.

In this paper, the feature extraction of static gestures based on EMG signals is studied. Although some theoretical and experimental results have been obtained, there are still many problems that can be further discussed. The selection of the original features, the specific choice of features and the combination of features need to be further studied; in addition to the method of transforming dimensionality reduction, the feature selection method can be used to reduce the dimension, but the specific algorithm needs to be further determined.

Acknowledgements This work was supported by Grants of National Natural Science Foundation of China (Grant Nos. 51575407, 51505349, 51575338, 51575412 and 61733011) and the Grants of National Defense Pre-research Foundation of Wuhan University of Science and Technology (GF201705).

Compliance with ethical standards

Conflict of interest The authors declare that they have no conflict of interest.

References

1. Ison M, Vujaklija I, Whitsell B et al (2016) High-density electromyography and motor skill learning for robust long-term control of a 7-DoF robot arm. IEEE Trans Neural Syst Rehabil Eng 24(4):424–433
2. Fang Y, Zhou D, Li K et al (2017) Interface prostheses with classifier-feedback-based user training. IEEE Trans Biomed Eng 64(11):2575–2583
3. Ding W, Li G, Sun Y et al (2017) D–S evidential theory on sEMG signal recognition. Int J Comput Sci Math 8(2):138–145
4. Falisse A, Van Rossom S, Jonkers I et al (2017) EMG-Driven Optimal Estimation of Subject-SPECIFIC Hill Model Muscle-Tendon Parameters of the Knee Joint Actuators. IEEE Transactions on Biomedical Engineering 64(9):2253–2262
5. Li Z, Li G, Sun Y et al (2017) Development of articulated robot trajectory planning. Int J Comput Sci Math 8(1):52–60
6. Farina D, Jiang N, Rehbaum H et al (2014) The extraction of neural information from the surface EMG for the control of upper-limb prostheses: emerging avenues and challenges. IEEE Trans Neural Syst Rehabil Eng 22(4):797–809
7. Chen D, Li G, Sun Y et al (2017) Fusion hand gesture segmentation and extraction based on CMOS sensor and 3D sensor. Int J Wirel Mob Comput 12(3):305–312
8. Miao W, Li G, Sun Y et al (2016) Gesture recognition based on sparse representation. Int J Wirel Mob Comput 11(4):348–356
9. Ding W, Li G, Jiang G et al (2015) Intelligent computation in grasping control of dexterous robot hand. J Comput Theor Nanosci 12(12):6096–6099
10. Tyagi P, Arora A, Rastogi V (2017) Stress analysis of lower back using EMG signal. Biomed Res 28(2):519–524
11. Jiang D, Zheng Z, Li G et al (2018) Gesture recognition based on binocular vision. Cluster Comput. https://doi.org/10.1007/s10586-018-1844-5
12. Shih JJ, Krusienski DJ, Wolpaw JR (2012) Brain-computer interfaces in medicine. Mayo Clin Proc 87(3):268–279
13. Chang W, Li G, Kong J et al (2018) Thermal mechanical stress analysis of ladle lining with integral brick joint. Arch Metall Mater 63(2):659–666
14. Farina D, Holobar A, Merletti R et al (2010) Decoding the neural drive to muscles from the surface electromyogram. Clin Neurophysiol 121(10):1616–1623
15. Chen D, Li G, Sun Y et al (2017) An interactive image segmentation method in hand gesture recognition. Sensors 17(2):253
16. Sun Y, Li C, Li G et al (2018) Gesture recognition based on kinect and sEMG signal fusion. Mob Netw Appl 23(4):797–805
17. Scheme E, Englehart K (2011) Electromyogram pattern recognition for control of powered upper-limb prostheses: state of the art and challenges for clinical use. J Rehabil Res Dev 48(6):643–659
18. Li G, Zhang L, Sun Y et al (2018) Towards the sEMG hand: internet of things sensors and haptic feedback application. Multimed Tools Appl. https://doi.org/10.1007/s11042-018-6293-x
19. Sensinger JW, Lock BA, Kuiken TA (2009) Adaptive pattern recognition of myoelectric signals: exploration of conceptual framework and practical algorithms. IEEE Trans Neural Syst Rehabil Eng 17(3):270–278

20. Sun Y, Hu J, Li G et al (2018) Gear reducer optimal design based on computer multimedia simulation. J Supercomput. https://doi.org/10.1007/s11227-018-2255-3
21. Elamvazuthi I, Duy NHX, Ali Z et al (2015) Electromyography (EMG) based classification of neuromuscular disorders using multi-layer perceptron. Procedia Comput Sci 76:223–228
22. Li G, Tang H, Sun Y et al (2017) Hand gesture recognition based on convolution neural network. Clust Comput. https://doi.org/10.1007/s10586-017-1435-x
23. He Y, Li G, Liao Y et al (2017) Gesture recognition based on an improved local sparse representation classification algorithm. Cluster Comput. https://doi.org/10.1007/s10586-017-1237-1
24. He Y, Li G, Sun Y et al (2018) Temperature intelligent prediction model of coke oven flue based on CBR and RBFNN. International Journal of Computing Science and Mathematics 9(4):327–339
25. Li B, Sun Y, Li G et al (2017) Gesture recognition based on modified adaptive orthogonal matching pursuit algorithm. Cluster Comput. https://doi.org/10.1007/s10586-017-1231-7
26. Xiong C, Chen W, Sun B et al (2016) Design and implementation of an anthropomorphic hand for replicating human grasping functions. IEEE Trans Rob 32(3):652–671
27. Li G, Liu J, Jiang G et al (2015) Numerical simulation of temperature field and thermal stress field in the new type of ladle with the nanometer adiabatic material. Adv Mech Eng 7(4):1687814015575988
28. Fang Y (2015) Interacting with prosthetic hands via electromyography signals. School of Computing University of Portsmouth
29. Jiang D, Li G, Ying Sun et al (2018) Gesture recognition based on skeletonization algorithm and CNN with ASL database. Multimed Tools Appl. https://doi.org/10.1007/s11042-018-6748-0
30. Cheng W, Sun Y, Li G et al (2018) Jointly network: a network based on CNN and RBM for gesture recognition. Neural Comput Appl. https://doi.org/10.1007/s00521-018-3775-8
31. Huang Z, Shan G, Chen J, Sun J (2018) TRec: an efficient recommendation system for hunting passengers with deep neural networks. Neural Comput Appl. https://doi.org/10.1007/s00521-018-3728-2
32. Fang Y, Liu H, Li G et al (2015) A multichannel surface EMG system for hand motion recognition. Int J Humanoid Robot. https://doi.org/10.1142/S0219843615500115
33. Wu B, Yan X, Wang Y, Soares C (2017) An Evidential Reasoning-Based CREAM to Human Reliability Analysis in Maritime Accident Process. Risk Analysis 37(10):1936–1957
34. Chen D, Li G, Kong J et al (2017) Hand gesture recognition using interactive image segmentation method. In: International conference on intelligent robotics and applications. Springer, Cham (2017). https://doi.org/10.1007/978-3-319-65289-4_51
35. Li G, Liu Z, Jiang G et al (2015) Numerical simulation of the influence factors for rotary kiln in temperature field and stress field and the structure optimization. Advances in Mechanical Engineering 7(6):1687814015589667
36. Liao Y, Sun Y, Li G et al (2017) Simultaneous calibration: a joint optimization approach for multiple kinect and external cameras. Sensors 17(7):1491
37. He Y, Li G, Zhao Y et al (2018) Numerical simulation-based optimization of contact stress distribution and lubrication conditions in the straight worm drive. Strength Mater 50(1):157–165
38. Tan C, Sun Y, Li G et al (2019) Research on Gesture Recognition of Smart Data Fusion Features in the IoT. Neural Comput Appl. https://doi.org/10.1007/s00521-019-04023-0
39. Li G, Miao W, Jiang G et al (2015) Intelligent control model and its simulation of flue temperature in coke oven. Discrete Contin Dyn Syst Ser S 8(6):1223–1237
40. Miao W, Li G, Jiang G et al (2015) Optimal grasp planning of multi-fingered robotic hands: a review. Appl Comput Math 14(3):238–247
41. Saeys Y, Inza I, Larrañaga P (2007) A review of feature selection techniques in bioinformatics. Bioinformatics 23(19):2507–2517
42. Li G, Qu P, Kong J et al (2013) Influence of working lining parameters on temperature and stress field of ladle. Appl Math Inf Sci 7(2):439–448
43. Chen D, Li G, Jiang G et al (2015) Intelligent computational control of multi-fingered dexterous robotic hand. J Comput Theor Nanosci 12(12):6126–6132
44. Mehmood T, Liland KH, Snipen L et al (2012) A review of variable selection methods in partial least squares regression. Chemometr Intell Lab Syst 118(16):62–69
45. Li G, Qu P, Kong J et al (2013) Coke oven intelligent integrated control system. Appl Math Inf Sci 7(3):1043–1050
46. Yin Q, Li G, Zhu J (2017) Research on the method of step feature extraction for EOD robot based on 2D laser radar. Discrete Contin Dyn Syst Ser S (DCDS-S) 8(6):1415–1421
47. Li G, Jiang D, Zhou Y et al (2019) Human Lesion Detection Method Based on Image Information and Brain Signal. IEEE Access 7:11533–11542
48. Du F, Sun Y, Li G et al (2017) Adaptive fuzzy sliding mode control algorithm simulation for 2-DOF articulated robot. Int J Wirel Mob Comput 13(4):306–313
49. Li G, Wu H, Jiang G et al (2019) Dynamic Gesture Recognition in the Internet of Things. IEEE Access 7(1):23713–23724
50. Luo B, Sun Y, Li G et al (2019) Decomposition algorithm for depth image of human health posture based on brain health. Neural Comput Appl. https://doi.org/10.1007/s00521-019-04141-9
51. Andersen CM, Bro R (2010) Variable selection in regression—a tutorial. J Chemom 24(11–12):728–737
52. Li G, Gu Y, Kong J et al (2013) Intelligent control of air compressor production process. Appl Math Inf Sci 7(3):1051–1058
53. Li G, Kong J, Jiang G et al (2012) Air-fuel ratio intelligent control in coke oven combustion process. Inf Int Interdiscip J 15(11):4487–4494
54. Zhang L, Zheng Z, Li G et al (2018) Tactile sensing and feedback in SEMG hand. Int J Comput Sci Math 9(4):365–376